



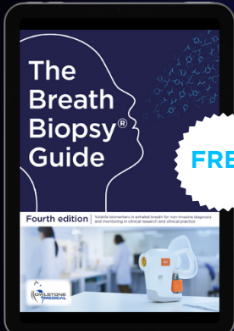
## A three-axis goniometer in an UHV molecular beam experiment

To cite this article: A Raukema *et al* 1997 *Meas. Sci. Technol.* **8** 253

View the [article online](#) for updates and enhancements.

### You may also like

- [Probe manipulators for Wendelstein 7-X and their interaction with the magnetic topology](#)  
M RACK, D HÖSCHEN, D REITER *et al.*
- [Determination method of dynamic characteristics of mobile terrestrial robotic complex manipulator](#)  
S V Strutynskiy
- [Path Planning Simulation of 6-DOF Manipulator](#)  
Junhao Zhang, Xingbo Yang, Yawei Li *et al.*



**FREE** **The Breath Biopsy® Guide**  
Fourth edition

[DOWNLOAD THE FREE E-BOOK](#)

BREATH BIOPSY®

OWLSTONE MEDICAL

The advertisement features a dark blue background with a white molecular structure pattern in the top right. On the left, a tablet displays the e-book cover for 'The Breath Biopsy Guide' (Fourth edition), which shows a person's profile and a medical device. A white starburst with the word 'FREE' is overlaid on the cover. To the right of the tablet, the title 'The Breath Biopsy® Guide' is written in large white font, with 'Fourth edition' in a smaller blue font below it. A blue button with white text says 'DOWNLOAD THE FREE E-BOOK'. At the bottom right, there are two logos: 'BREATH BIOPSY®' in an orange box and 'OWLSTONE MEDICAL' in a white box with a blue owl icon.

# A three-axis goniometer in an UHV molecular beam experiment

A Raukema, A P de Jongh, H P Alberda, R Boddenberg,  
F G Giskes, E de Haas, A W Kleyn, H Neerings, R Schaafsma  
and H Veerman

FOM-Institute for Atomic and Molecular Physics, Kruislaan 407,  
1098 SJ Amsterdam, The Netherlands

Received 26 June 1996, accepted for publication 17 December 1996

**Abstract.** A sample manipulator with six degrees of freedom, which is part of a molecular beam scattering apparatus used to study gas–surface interactions, is described. Incidence parameters such as the angle of incidence and the azimuthal angle can be set and particles leaving the surface both in and out the plane of incidence can be measured (to within  $0.1^\circ$  accuracy). The latter is achieved, under computer control, by a combination of the movement of the manipulator and the movement of the detector. Cooling of the sample to liquid  $N_2$  temperatures and heating to at least 1600 K is possible. A mathematical relation among the positions of the manipulator and of the detector, the required incidence angle of the particles and the final angle of the scattered particles to be measured is derived.

## 1. Introduction

One of the ways to study molecule–surface interactions is to aim a beam of molecules at a surface and to analyse the scattered particles or measure the fraction of the incident molecules that adsorb at the surface. Several experimental parameters can be varied to gain information on the interaction such as the energy (translational and/or internal) of the incident molecules, the surface temperature, the orientation of the molecules with respect to the sample surface, the incidence angle of the molecules, the crystallographic direction along which the molecules approach the sample surface and the angles measured with respect to the surface normal and to the plane of incidence under which the scattered particles are detected (final or detection angles).

The molecules leaving the surface can be analysed using a time-of-flight (TOF) technique. Detection of the molecules can be achieved with a (differentially pumped) mass spectrometer or an internal-state-sensitive detection technique such as resonance-enhanced multiphoton ionization (REMPI). Sticking probabilities can be measured by monitoring the residual gas pressure while exposing the surface to the molecular beam or by monitoring the specular He reflectivity while dosing. Desorbing the adsorbed molecules by ramping the surface temperature (temperature programmed desorption (TPD)) after exposing the surface to the molecular beam can also be used to determine the sticking probability, discriminate between different adsorption states and give information on desorption energies and pre-exponential factors.

The above certainty is not a full list of the capabilities of a molecular beam system but gives an overview of the

possibilities of our system in which the sample manipulator plays a vital role. In the present paper a sample manipulator which allows for the options mentioned will be described. The option of detecting particles scattered out of the plane of incidence as is allowed by the manipulator is one of the unique features of our set-up. A coupled movement in the degrees of freedom of the manipulator and of the detector has to be performed to set the incidence and the detection angles. The mathematical relations describing these couplings and expressing the manipulator and detector positions as functions of the incidence and detection angles are derived.

## 2. The experimental set-up

The experimental set-up consists of two molecular beam lines connected to an UHV chamber in which a sample is mounted. A molecular or atomic beam is generated by the supersonic expansion of a gas from a nozzle in the beam line. One of the beam lines extends into the UHV chamber to keep the distance between the nozzle and the sample as short as possible for a maximum particle flux at the sample. A drawing of the UHV chamber and this beam line is shown in figure 1 [1]. The other beam line was added at a later time and is especially designed for experiments with oriented nitric oxide (NO) molecules [2]. Both beam lines are differentially pumped.

The sample is mounted on a manipulator in the centre of the UHV chamber. A differentially pumped quadrupole mass spectrometer (QMS) [1] and a REMPI detector for measuring rovibrationally excited molecules [3] can rotate in a horizontal plane around the sample. Both detectors

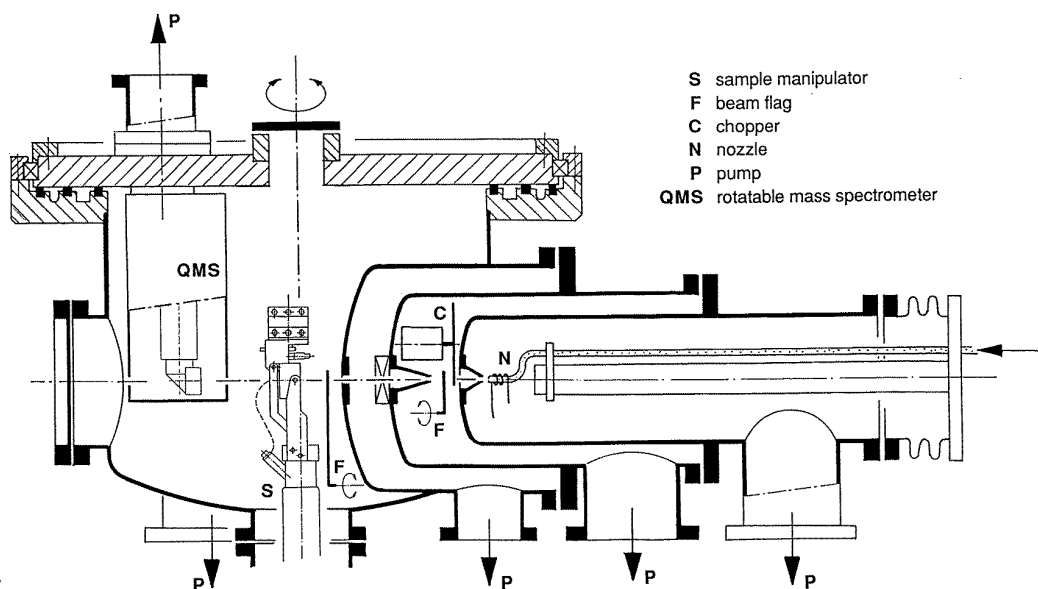


**Figure 1.** An overview of the experimental set-up. It shows a molecular beam line and the scattering chamber. The described manipulator is seen connected to the bottom of the scattering chamber. The cover of the UHV chamber can be rotated.

are connected to the cover of the UHV chamber, which is rotatable. UHV is maintained while rotating the cover by doubly differentially pumping the seal between the cover and rest of the chamber. The seal consists of three spring-loaded Teflon seals and two pumping stages.

For surface characterization the system is equipped to perform Auger electron spectroscopy (AES) and low-energy electron diffraction (LEED). A residual gas analyser (RGA) is present for monitoring the background pressure and there is an ion sputter gun for cleaning the sample. To allow exchange of samples without breaking the UHV, a sample exchange chamber is also connected to the scattering chamber.

The former two-axis sample manipulator is replaced by the three-axis manipulator described. Since no commercial manipulator that satisfied our demands was available we developed one ourselves.

### 3. The design criteria

In a surface scattering or sticking experiment control is required both over the angle of incidence of the incident beam, measured with respect to the surface normal, and also over the azimuthal angle. The azimuthal angle is defined as the angle between a chosen crystallographic direction on the surface and the plane of incidence of the particle, which is the plane through the surface normal and the incidence trajectory of the particle (see figure 2). One should also have control over the angles, both in and out of the plane of incidence, under which scattered particles are detected. Since our detector can only rotate in one plane it should be possible to rotate (tilt) the sample such that control of out-of-plane scattering is also obtained. It is obvious that the incidence and final angles of the particles referenced to a frame connected to the sample will not be the same as

the angles describing the sample and the detector position referenced to a frame connected to the experimental set-up.

It should be possible to face the sample towards the molecular beam, but also towards the surface analytical LEED and AES installations, an ion sputter gun and a sample exchange chamber which are positioned in the detector plane in an almost full circle around the sample. The manipulator should be retractable from the beam path to allow characterization of the incident beam.

Sample positioning should be motor-driven and computer-controlled. The desired accuracy in the positioning of the sample is only moderate: for the rotations  $\pm 0.1^\circ$  and for the translations  $\pm 0.1$  mm is sufficient. A  $360^\circ$  polar rotation ( $\theta_p$ ) of the sample manipulator around a vertical axis of the experimental set-up, a tilt rotation ( $\theta_T$ ) of the sample with respect to the (horizontal) detector plane ( $90^\circ$  tilt backwards an  $20^\circ$  forwards), a  $360^\circ$  spin rotation ( $\theta_S$ ) of the sample around the surface normal and a  $\pm 15$  mm  $X$ ,  $Y$  and  $Z$  translation of the sample manipulator with respect to the centre of the experiment are required.

It should be possible to cool the sample to about liquid  $N_2$  temperature and heat it to about 1200 K. Both radiative heating and heating by electron bombardment of the sample are required. The last method gives the option of fast heating rates of the sample for TPD experiments. To avoid a large heat load on the sample surroundings the sample should be thermally isolated at elevated temperatures. The sample should also be electrically insulated from its surroundings. In this way it is possible to connect it to earth potential or to bias it positively or negatively.

Samples should be easily exchanged, preferably without breaking the vacuum, but rather using the sample exchange chamber. It should also be possible to perform experiments with oriented NO. To do so, a strong electrical field is employed in which the NO molecules orient due the Stark effect [2]. An orientation electrode in front of the (earthed)

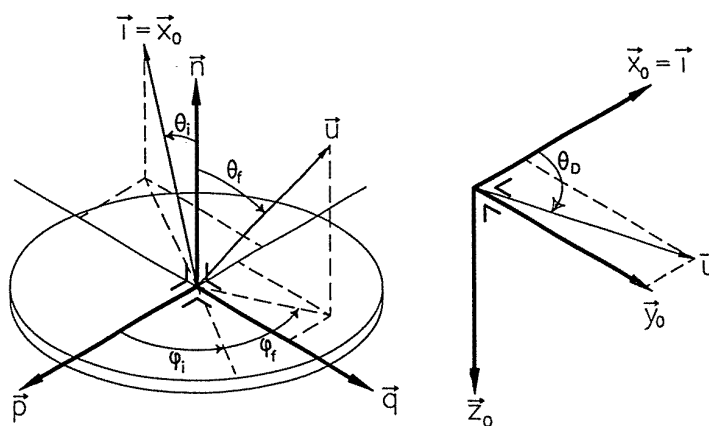


**Figure 2.** Incidence and exit vectors describing the incident and scattered particles in terms of the angles  $\theta_i$ ,  $\phi_i$ ,  $\theta_f$  and  $\phi_f$  in the basis set  $(n, p, q)$  and as functions of  $\theta_D$  in the basis set  $(x_0, y_0, z_0)$ . The vector  $p$  is defined to be along a high-symmetry line on the surface,  $n$  is the surface normal. The vector  $x_0$  points in the direction of the molecular beam line and the vector  $z_0$  points downwards and is perpendicular to the detector plane.

sample should therefore be provided for. The electrode must be movable so that it can be put into a position where it does not interfere with other experiments or sample exchange.

The manipulator should be mounted on an 8 inch outer diameter flange in the bottom of the experimental set-up. The space available in the experiment is limited. Only 65 mm is available between one of the beam lines and the centre of the UHV chamber. Since the demand on polar rotation is a full  $360^\circ$ , the top of the manipulator should not occupy more space than fits in a cylinder with 65 mm radius. Positioning of a beam flag for sticking probability measurements [4, 5] between the sample and the beam line in the UHV chamber should be possible. In the vertical direction no limitations of this order are imposed. The detector used for REMPI experiments is very close to the sample in these experiments in order not to lose intensity and it should not be obstructed by the manipulator. Incident and scattered/desorbing particles should also not be obstructed by parts of the manipulator (except for the orientation electrode).

A last important constraint on the design is UHV compatibility. In the following sections a description of the manipulator will be given and the relation among the manipulator position and the incidence and final angles of incident and scattered particles will be derived.

#### 4. The implementation of the system

The newly designed sample manipulator is based on a Fisons Omniax MXY25 and MXZ100 high-precision  $X$ - $Y$  translation and  $Z$  translation stage. It consists, as is shown in figure 3, of a wide-bore bellows  $X$ - $Y$  stage on which a 100 mm bellows for the  $Z$  movement is mounted. The  $Z$  movement bellows ends in another flange on which a Fisons DPRF55 differentially pumped rotational feed-through is mounted. Through this rotational feed-through and through the  $Z$  bellows there runs a 50 mm diameter column. One end of this column is a 4.5 inch flange,

which is connected to the rotational feed-through. On the other side of this flange there is a piece with several ports allowing for the connection of liquid  $N_2$  tubing and several electrical feed-throughs. At the bottom a Fisons SLMD100 linear translator stage is mounted, closing this end of the manipulator. The column moves at the top of the  $X$ - $Y$  stage through a bearing allowing both for polar rotation ( $\theta_p$ ) and for  $Z$  translation.

On top of the column there is mechanism allowing for the tilt ( $\theta_T$ ) and spin rotation ( $\theta_S$ ) and a push rod connected to the linear translation stage moves, through the column, the tilt rotation of the sample. This part is shown enlarged on the left-hand side of the figure 3 and photos are shown in figure 4. A housing is mounted via two small ball bearings and in between two arms on the column. The push rod is connected via two rotation centres to the housing and allows, by moving up or down, for the tilt rotation of the housing. In the housing the sample holder is put in a slide bearing allowing for spinning the sample holder and thus the sample. Spin rotation of the holder is done by the model B23.1 UHV compatible stepper motor from Arun Microelectronic Limited (AML). The stepper motor is mounted on top of the housing. A 10:1 gear connection reduces the sample holder rotation speed with respect to the stepper motor rotation speed. The sample holder can be removed from the housing via a sample exchange rod to transport it to the sample exchange chamber. In the back of the housing, in an alumina plate, there are five connectors into which five pins of the sample holder are pushed. These allow for electrical connections: two for the filament for heating the sample, one electrical connection to the sample and two for a K-type thermocouple. A drawing of the sample holder in a housing is shown in figure 5. All the electrical wiring for the manipulator in UHV is also put through the column and ends in an alumina plate with connectors.

A piece of Cu-Cr is mounted on the alumina plate in the housing. A Mo plate mounted at the back of the sample holder fits loosely into this Cu-Cr piece. On the other side of the Cu-Cr piece is clamped a set of Cu braids connected

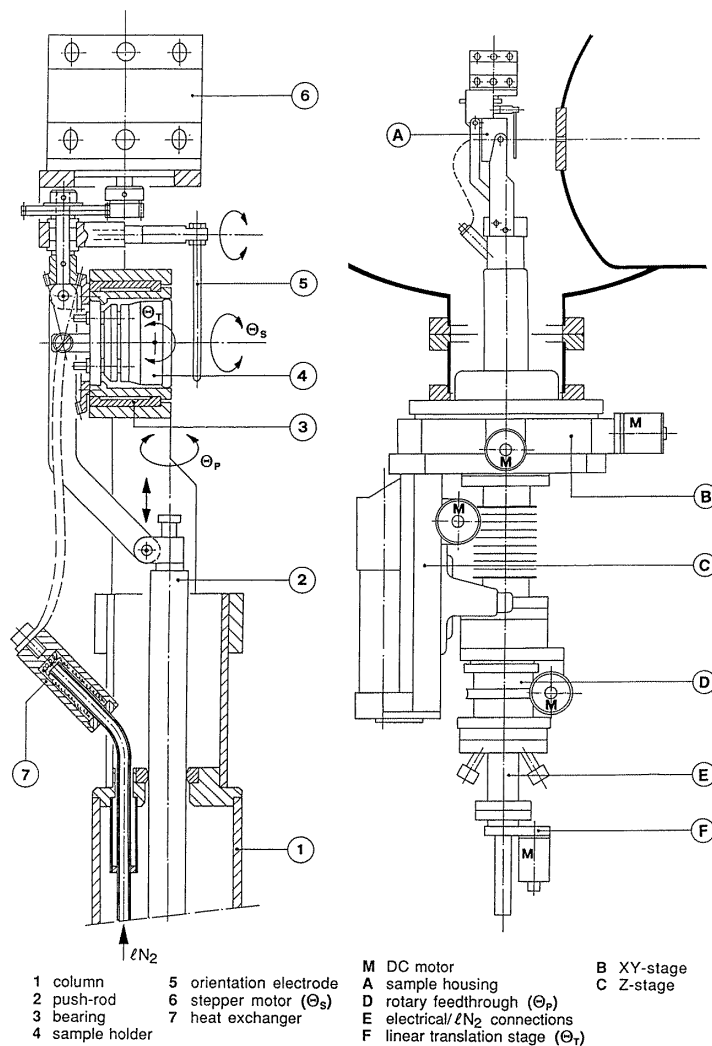


**Figure 3.** A drawing of the sample manipulator as it is mounted in the experimental set-up is shown on the right-hand side. The top of the manipulator allowing for the tilt and spin rotation is shown enlarged on the left-hand side.

to a heat exchanger. Since Cu–Cr has a larger expansion coefficient than Mo, the sample holder will make thermal contact when cooling. In this way a cooling connection is made to the sample. For good thermal heat contact the Cu braids are electron-beam welded into two Cu blocks. One is clamped on the Cu–Cr piece, the other one on the liquid N<sub>2</sub> heat exchanger (not shown exactly in figure 3). Flexible Cu braids are used to allow for the tilt and spin rotation of the sample.

In the sample holder the sample is clamped onto a Cu–Cr block with sapphire insulation in between. The sapphire acts as an electrical insulation for the sample, but also as a heat diode. At low temperatures it has a large heat conductivity and at high temperatures a low one. In this way the sample is thermally insulated at high temperatures and it can be cooled via the copper block. A tungsten filament for heating is mounted behind the sample. When applying electron-beam bombardment heating, all the electrons should hit the sample in order not to heat the surroundings. Therefore the heat screen behind the filament is at the same potential as the filament and a +25 V bias is

applied to the sample. Linear heating rates up to 20 K s<sup>-1</sup> have been attained and were limited only by the temperature controller used [7]. A sample temperature of  $T_s = 120$  K is attained after cooling for about 1 h [6]. Cooling of the sample takes of the order of minutes after flashing it from a low temperature to a temperature of about 800 K. In a high-temperature version of the sample holder in which the Cu–Cr block is replaced by a Mo block a temperature of over 1600 K can be attained (measured with a C-type thermocouple).

An orientation electrode is mounted on the block in between the sample holder housing and the stepper motor. It can be moved in and out of position with the aid of the sample-exchange rod.

The motors for all except the spin rotation are mounted outside the vacuum. They are all DC motors and their positions are given by Hewlett-Packard HEDS-5010/6010 optical increment encoders mounted on the back of the motors. The controllers for these motors keep track of the position in encoder steps with respect to a reference position. If the position is lost somehow, the reference

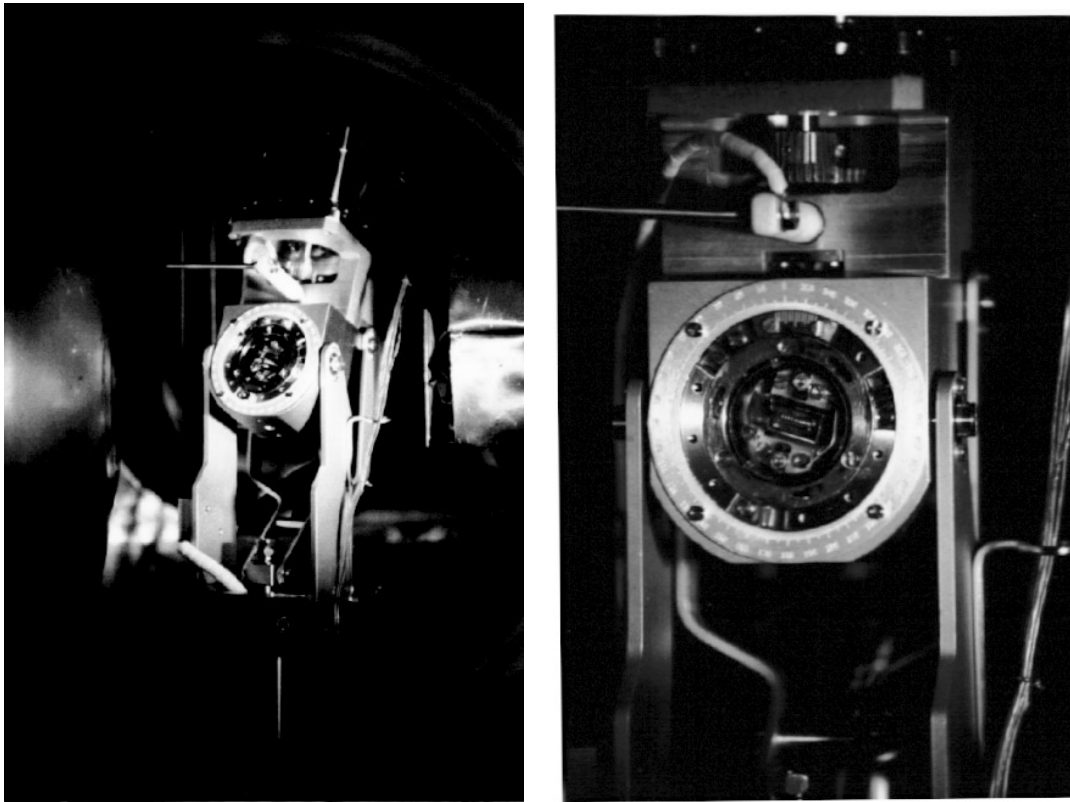


**Figure 4.** The left-hand photograph shows the top of the manipulator slightly tilted and the right-hand photograph is a close-up of the housing for the sample holder with the sample holder in. A sample is not mounted, which makes the heating filament visible.

position can easily be found again by reference to optical marks which can be traced with the aid of Hewlett-Packard HBCS-1100 optical sensors. The resolution of the encoders in combination with the gear boxes used and the reproducibility of the Fisons components is far better than the accuracy required and will not be evaluated further. For the spin rotation the accuracy in the position is given by the steps of the stepper motor and the reduction and backlash in the gears. Since the steps of the stepper motor are  $1.8^\circ$  and the reduction 10:1, the accuracy of the position, disregarding the backlash, will be  $\pm 0.1^\circ$ . The backlash is estimated to be  $0.1^\circ$  also, giving an accuracy in the spin rotation position of  $\pm 0.2^\circ$ . No encoder is used for the stepper motor. The spin position would be in error if steps were lost in spinning the sample. Loss of steps is not expected since the torque of the stepper motor is rather large. The controller supplied with the stepper motor keeps track of the spin position in steps with respect to a reference. The reference can be read by the human eye using a telescope from a precision scale mounted on front of the housing of the sample holder.

The three rotational axes of the sample manipulator are positioned such that the  $\theta_T$  axis is perpendicular to the  $\theta_P$  axis and the  $\theta_S$  axis perpendicular to the  $\theta_T$  axis. Both the  $\theta_P$  axis and the  $\theta_S$  axis are designed to go through the centre of the sample surface. The  $\theta_S$  axis is designed to be perpendicular to the sample surface. If the thickness of the sample used is larger or smaller than the value fixed in the manipulator design or when the back and front surface of

the sample are not parallel this will no longer hold. When moving the manipulator one should correct for the sample thickness. If the  $X$ - $Y$  plane of the manipulator is not parallel with the  $X$ - $Y$  plane of the experiment (the plane of the detector), which is the case by approximately  $2^\circ$  in our experiment, one should also correct for this when positioning the sample. The  $\theta_T$  axis is designed to lie behind the sample surface, which thus will move out of the centre of the experiment when the sample is being tilted; the tilt of the sample is coupled to the  $XYZ$  coordinates of the manipulator. One should also correct for this. A linear translation drives the  $\theta_T$  rotation and a relation between the translation and the angle  $\theta_T$  is derived. This is easily done with the dimensions of the different parts employed in the tilt movement.

The cover to which the detectors are attached is moved by a large-torque DC motor and its position is read via a Sony PL-20 magnetic ruler and read-out unit. The resolution is far better than the error of  $0.1^\circ$  in finding the maximum intensity of the direct beam, which is a reference for the alignment.

Calibrations of the different degrees of freedom are carried out by moving the manipulator positions over a certain distance or angle and reading the number of increments or the encoders of the stepper motor. These calibrations are set in the computer program controlling the manipulator and also the zero position can be set. In this way the sample manipulator is easily positioned. Finding the zero positions is done with the aid of a He-Ne

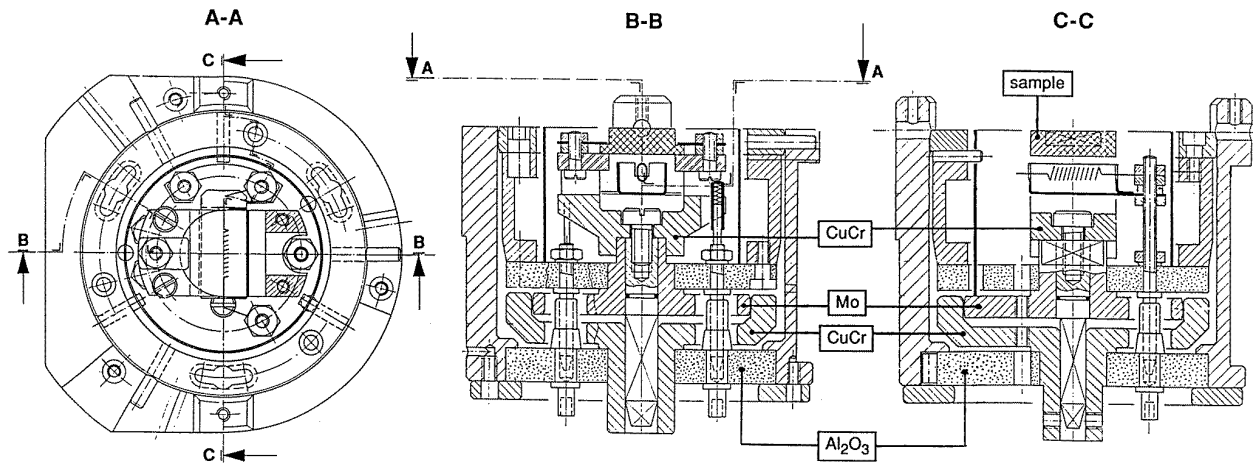


Figure 5. The sample holder for easy sample exchange drawn in its housing.

laser directed through the molecular beam and (specularly) reflecting from the surface and with the aid of specular helium atom reflectivity. It is estimated that the zero position can be found in this way with about  $0.2^\circ$  and 0.5 mm accuracy for the different degrees of freedom. The facts that the  $X$ - $Y$  plane of the manipulator and of the detector and that the back and front planes of the sample are not parallel can also be traced using these reflections.

## 5. Moving the manipulator and detector

The angles describing the particles incident on and scattered from the surface ( $\theta_i$ ,  $\phi_i$ ,  $\theta_f$  and  $\phi_f$ ) are not the same as the angles describing the position of the sample and detector ( $\theta_p$ ,  $\theta_T$ ,  $\theta_S$  and  $\theta_D$ ). To be able to position the sample and detector for a specified scattering geometry, a relation between the two sets of angles must be derived. Before we can do so, both sets of angles have to be defined.

Both the incidence and the exit vector of the incident and scattered particles, respectively, are described by two angles. The incidence vector is defined as pointing in the direction of the nozzle, opposite to the direction of the incidence particles. The exit vector is defined as pointing in the direction in which the particles are scattered, in the direction of the detector. The angle between a vector and the surface normal is referred to as  $\theta$ , and the angle between the projection of a vector on the surface and some reference direction on the surface is referred to as  $\phi$ . Figure 2 is a drawing of these vectors and angles. The reference direction on the surface for the incident particles is a high-symmetry direction, indicated by the vector  $p$  in figure 2. For the scattered particles the reference is the plane of incidence, defined through the surface normal  $n$  and the incidence vector  $i$ . The vector  $q$  is defined such that the vector set  $(n, p, q)$  constitutes a right-handed basis set [8] that is connected to the sample surface.  $\theta_i$  and  $\phi_i$  are the angles for the incident particles and  $\theta_f$  and  $\phi_f$  those for the scattered particles. With these angles the incidence vector  $i$  and exit vector  $u$  can be described in coordinates referring

to the basis set  $(n, p, q)$ :

$$i = \begin{pmatrix} \cos \theta_i \\ -\sin \theta_i \cos \phi_i \\ -\sin \theta_i \sin \phi_i \end{pmatrix}_{(n,p,q)}$$

$$u = \begin{pmatrix} \cos \theta_f \\ \sin \theta_f \cos(\phi_f + \phi_i) \\ \sin \theta_f \sin(\phi_f + \phi_i) \end{pmatrix}_{(n,p,q)}. \quad (1)$$

The four angles are defined to be in the ranges

$$0 \leq \theta_i, \theta_f < 90^\circ \quad -180^\circ < \phi_i, \phi_f \leq 180^\circ. \quad (2)$$

Particles that have trapped at the surface and desorb again in a scattering experiment are described by characteristics (energy, temperature and intensity) that are dependent only on  $\theta_f$  and not on  $\phi_f$ . Defining those two angles in a way other than that described above leads to a less obvious description of these characteristics in terms of the scattering angles.

The position of the sample is described in terms of three angles: the polar rotation angle  $\theta_p$  the tilt rotation angle  $\theta_T$  and the spin rotation angle  $\theta_S$ . Together with the rotation angle  $\theta_D$  of the detector this gives another four angles describing the positions of the sample and the detector. Both the angles  $\theta_p$  and  $\theta_D$  are described with respect to a coordinate system connected to our scattering apparatus. The basis set  $(x_0, y_0, z_0)$  is chosen in such a way that the vector  $x_0$  points in the direction of the nozzle source and is thus identical to the incidence vector  $i$ . Both the vectors  $x_0$  and  $y_0$  are in the detection plane, the plane in which our detector rotates, and  $y_0$  points in such a direction that  $\theta_D$  is positive for attainable detector positions. The vector  $z_0$  is chosen to provide a right-handed basis set  $(x_0, y_0, z_0)$  and is pointing down for our set-up. Incidence and exit vectors are described in this set as

$$i = \begin{pmatrix} 1 \\ 0 \\ 0 \end{pmatrix}_{(x_0, y_0, z_0)} \quad u = \begin{pmatrix} \cos \theta_D \\ \sin \theta_D \\ 0 \end{pmatrix}_{(x_0, y_0, z_0)} \quad (3)$$

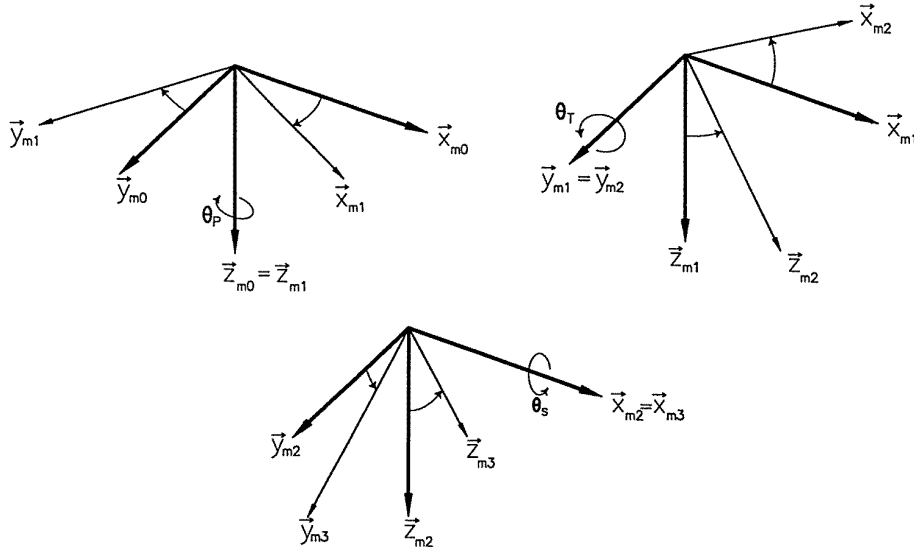


**Figure 6.** Successive rotations of the sample manipulator (see equation (5)).

with the detector angle  $\theta_D$  measured with respect to the vector  $\mathbf{x}_0$ . In a scattering experiment

$$0 \leq \theta_D \leq 180^\circ \quad (4)$$

will hold but in practice the interval will be smaller because the detector cannot reach all positions. For our experimental set-up  $58^\circ \leq \theta_D \leq 180^\circ$  holds.

The polar rotation angle  $\theta_P$  is the rotation of the manipulator around the vector  $\mathbf{z}_{m0}$ , of a basis set  $(\mathbf{x}_{m0}, \mathbf{y}_{m0}, \mathbf{z}_{m0})$  connected to the sample manipulator. With this rotation we define the transformation  $\mathcal{R}_{z_{m0}}(\theta_P)$  to another basis set  $(\mathbf{x}_{m1}, \mathbf{y}_{m1}, \mathbf{z}_{m1})$ , with  $\mathbf{z}_{m0}$  of course identical to  $\mathbf{z}_{m1}$ . These rotations are shown in figure 6. The tilt axis of the manipulator is through the vector  $\mathbf{y}_{m1}$  after the transformation  $\mathcal{R}_{z_{m0}}(\theta_P)$ . Performing a tilt rotation of the sample defines another rotation transformation  $\mathcal{R}_{y_{m1}}(\theta_T)$  to the basis set  $(\mathbf{x}_{m2}, \mathbf{y}_{m2}, \mathbf{z}_{m2})$ , with  $\mathbf{y}_{m1}$  identical to  $\mathbf{y}_{m2}$ . A spin rotation leads to the rotation transformation  $\mathcal{R}_{x_{m2}}(\theta_S)$  to the basis set  $(\mathbf{x}_{m3}, \mathbf{y}_{m3}, \mathbf{z}_{m3})$ . If the sample is mounted in the manipulator in such a way that the surface normal  $\mathbf{n}$  coincides with the spin rotation axis, thus if  $\mathbf{n} = \mathbf{x}_{m3} = \mathbf{x}_{m2}$  and the set  $(\mathbf{x}_{m0}, \mathbf{y}_{m0}, \mathbf{z}_{m0})$  connected to the manipulator coincides with the set  $(\mathbf{x}_0, \mathbf{y}_0, \mathbf{z}_0)$  connected to the scattering chamber, then we have defined the transformation

$$\mathcal{R} = \mathcal{R}_{x_{m2}(=\mathbf{n})}(\theta_S) \mathcal{R}_{y_{m1}}(\theta_T) \mathcal{R}_{z_{m0}(=\mathbf{z}_0)}(\theta_P) \quad (5)$$

from the basis set  $(\mathbf{x}_0, \mathbf{y}_0, \mathbf{z}_0)$  to the basis set  $(\mathbf{n}, \mathbf{p}, \mathbf{q})$  with these three rotations. The rotation transformations can be expressed in terms of the well-known rotation matrices [8]

$$\mathcal{R}_{z_{m0}}(\theta_P) = \begin{pmatrix} \cos \theta_P & \sin \theta_P & 0 \\ -\sin \theta_P & \cos \theta_P & 0 \\ 0 & 0 & 1 \end{pmatrix}$$

$$\mathcal{R}_{y_{m1}}(\theta_T) = \begin{pmatrix} \cos \theta_T & 0 & -\sin \theta_T \\ 0 & 1 & 0 \\ \sin \theta_T & 0 & \cos \theta_T \end{pmatrix}$$

$$\mathcal{R}_{x_{m2}}(\theta_S) = \begin{pmatrix} 1 & 0 & 0 \\ 0 & \cos \theta_S & \sin \theta_S \\ 0 & -\sin \theta_S & \cos \theta_S \end{pmatrix}. \quad (6)$$

With the aid of the transformation  $\mathcal{R}$ , the expression for the incidence vector  $\mathbf{i}$  and exit vector  $\mathbf{u}$  in the basis set  $(\mathbf{x}_0, \mathbf{y}_0, \mathbf{z}_0)$  can be transformed to the expression in the basis set  $(\mathbf{n}, \mathbf{p}, \mathbf{q})$ . By doing so a relation is derived between the angles  $\theta_P, \theta_T, \theta_S$  and  $\theta_D$  on the one hand and the angles  $\theta_i, \phi_i, \theta_f$  and  $\phi_f$  on the other. It turned out to be easier to work with the inverse transformation:

$$\mathcal{R}^{-1} \begin{pmatrix} \cos \theta_i \\ -\sin \theta_i \cos \phi_i \\ -\sin \theta_i \sin \phi_i \end{pmatrix}_{(\mathbf{n}, \mathbf{p}, \mathbf{q})} = \begin{pmatrix} 1 \\ 0 \\ 0 \end{pmatrix}_{(\mathbf{x}_0, \mathbf{y}_0, \mathbf{z}_0)} \quad (7)$$

$$\mathcal{R}^{-1} \begin{pmatrix} \cos \theta_f \\ \sin \theta_f \cos(\phi_f + \phi_i) \\ \sin \theta_f \sin(\phi_f + \phi_i) \end{pmatrix}_{(\mathbf{n}, \mathbf{p}, \mathbf{q})} = \begin{pmatrix} \cos \theta_D \\ \sin \theta_D \\ 0 \end{pmatrix}_{(\mathbf{x}_0, \mathbf{y}_0, \mathbf{z}_0)}. \quad (8)$$

Since the transformation  $\mathcal{R}$  is made up of multiple rotation transformations which are orthogonal,  $\mathcal{R}$  is also orthogonal. The inverse matrix of the transformation is then easily found because it is equal to the transpose matrix  $\mathcal{R}^{-1} = \mathcal{R}^T$ . The easiest way to the solution is now to take the equations resulting from the second and third components of equation (7) and the third component of equation (8) (right-hand sides 0) and, solving these together with the identity of the expression for the vector dot product of  $\mathbf{i}$  and  $\mathbf{u}$  in both basis sets  $(\mathbf{n}, \mathbf{p}, \mathbf{q})$  and  $(\mathbf{x}_0, \mathbf{y}_0, \mathbf{z}_0)$ , one obtains

$$(\mathbf{i} \cdot \mathbf{u})_{(\mathbf{n}, \mathbf{p}, \mathbf{q})} \equiv (\mathbf{i} \cdot \mathbf{u})_{(\mathbf{x}_0, \mathbf{y}_0, \mathbf{z}_0)}. \quad (9)$$

The latter leads to the expression for the detector angle

$$\theta_D = \arccos(\cos \theta_f \cos \theta_i - \sin \theta_i \sin \theta_f \cos \phi_f). \quad (10)$$

Under the constraint of detecting particles out of the plane of incidence with a constant angle between incident



and scattered particles [1], thus with a constant detector angle  $\theta_D$ , both the angles  $\theta_f$  and  $\phi_f$  have to be varied. Their relation is then given by

$$\theta_f = 2 \arctan \left[ \frac{-\sin \theta_i \cos \phi_f + (\sin^2 \theta_i \cos^2 \phi_f - \cos^2 \theta_D + \cos^2 \theta_i)^{1/2}}{\cos \theta_D + \cos \theta_i} \right]^{-1} \quad (11)$$

or

$$\phi_f = \pm \left[ \pi - \arccos \left( \frac{\cos \theta_D - \cos \theta_f \cos \theta_i}{\sin \theta_i \sin \theta_f} \right) \right]. \quad (12)$$

In the analysis as described it is assumed that the surface normal  $\mathbf{n}$  coincides with the vector  $\mathbf{x}_{m3}$ , but also that the polar rotation axis of the manipulator coincides with the vector  $\mathbf{z}_0$  (perpendicular to the scattering plane). If both assumptions are not true another four rotations have to be introduced. The assumptions do not hold if the  $X$ - $Y$  plane of the experiment (the detector plane) does not coincide with the  $X$ - $Y$  plane of the manipulator and if the front and the back plane of the sample are not parallel. First the vector coordinates expressed in the set  $(\mathbf{x}_0, \mathbf{y}_0, \mathbf{z}_0)$  have to be transformed to a basis set for which the vector  $\mathbf{z}$  coincides with the polar rotation axis of the manipulator  $\mathbf{z}_{m0}$ , which can be done with two rotations  $\alpha$  and  $\beta$ . Then the three manipulator rotation transformations can be performed followed by two rotations  $\gamma$  and  $\delta$  to make the vector  $\mathbf{x}_{m3}$  coincide with the surface normal. The transformation  $\mathcal{R}$  is now written as

$$\mathcal{R} = \mathcal{R}_{z_6}(\delta) \mathcal{R}_{y_{m3}}(\gamma) \mathcal{R}_{x_{m2}}(\theta_S) \mathcal{R}_{y_{m1}}(\theta_T) \mathcal{R}_{z_{m0}}(\theta_P) \times \mathcal{R}_{x_1}(\beta) \mathcal{R}_{y_0}(\alpha) \quad (13)$$

and it should be noted that equations (7) and (8) are still valid for the last expression for  $\mathcal{R}$ .

Evaluating the second and third components of equation (7) and the third component of equation (8) (right-hand sides 0) leads to the expressions

$$\begin{aligned} & \cos \theta_T \tan \theta_P - \tan \theta_i \sin \theta_T \tan \theta_P \sin(\theta_S + \phi_i) \\ & - \tan \theta_i \cos(\theta_S + \phi_i) \\ & = A(\alpha, \beta, \gamma, \delta, \theta_P, \theta_T, \theta_S, \theta_i, \phi_i, \theta_f, \phi_f) \end{aligned} \quad (14)$$

$$\begin{aligned} & \tan \theta_i \sin(\theta_S + \phi_i) - \tan \theta_T \\ & = B(\alpha, \beta, \gamma, \delta, \theta_P, \theta_T, \theta_S, \theta_i, \phi_i, \theta_f, \phi_f) \end{aligned} \quad (15)$$

$$\begin{aligned} & \tan \theta_T - \tan \theta_f \sin \phi_f \cos(\theta_S + \phi_i) \\ & - \tan \theta_f \cos \phi_f \sin(\theta_S + \phi_i) \\ & = C(\alpha, \beta, \gamma, \delta, \theta_P, \theta_T, \theta_S, \theta_i, \phi_i, \theta_f, \phi_f). \end{aligned} \quad (16)$$

Solving these equations gives the solutions for the sample manipulator angles:

$$\theta_S = -\phi_i + \arctan \left( \frac{\tan \theta_f \sin \phi_f + B(\dots) + C(\dots)}{\tan \theta_i - \tan \theta_f \cos \phi_f} \right) \quad (17)$$

$$\theta_T = \arctan[\tan \theta_i \sin(\theta_S + \phi_i) - B(\dots)] \quad (18)$$

$$\theta_P = \arctan \left( \frac{\tan \theta_i \cos(\theta_S + \phi_i) + A(\dots)}{\cos \theta_T - \tan \theta_i \sin \theta_T \sin(\theta_S + \phi_i)} \right). \quad (19)$$

Finding the solutions is straightforward, but all the mathematics involved is extremely tedious. We used a formula-manipulation software package (Waterloo Maple Software, University of Waterloo) to solve the problem. In the case of  $\phi_f = 0$ , thus measuring in the plane of incidence, and  $A = B = C = 0$ , it can be seen that

the different equations reduce to  $\theta_S = -\phi_i$ ,  $\theta_T = 0$ ,  $\theta_P = \theta_i$  and  $\theta_D = \theta_i + \theta_f$ .  $A = B = C = 0$  holds if  $\alpha = \beta = \delta = \gamma = 0^\circ$ .

In the case of the angles  $\alpha = \beta = \gamma = \delta = 0^\circ$  (thus  $A = B = C = 0$ ) equations (14)–(16) are identical to the ones found by solving equations (7) and (8) with the transformation as defined by equation (5). However, the expressions (14)–(16) are not exact because they could only be obtained under the assumptions  $\sin \alpha \approx \alpha$ ,  $\cos \alpha \approx 1$ ,  $\sin \beta \approx \beta$ ,  $\dots$  and  $\cos \delta \approx 1$  (with  $\alpha$ ,  $\beta$ ,  $\gamma$  and  $\delta$  expressed in radians). This assumption is only valid for small angles  $\alpha$ ,  $\beta$ ,  $\gamma$  and  $\delta$ , as will be fulfilled in practice. The values of  $A$ ,  $B$  and  $C$  will also be small under these circumstances.

Since  $A$ ,  $B$  and  $C$  are also expressed in the angles  $\theta_P$ ,  $\theta_T$  and  $\theta_S$  to be calculated, an iterative process is used to find the values for these sample-manipulator angles for a given scattering geometry ( $\theta_i$ ,  $\phi_i$ ,  $\theta_f$  and  $\phi_f$ ) and known angles  $\alpha$ ,  $\beta$ ,  $\gamma$  and  $\delta$ . One starts by taking  $A = B = C = 0$  and calculating  $\theta_P$ ,  $\theta_T$  and  $\theta_S$ . Then  $A$ ,  $B$  and  $C$  are calculated after which a new value for  $\theta_P$ ,  $\theta_T$  and  $\theta_S$  can be obtained. These last two steps are repeated until values for  $\theta_P$ ,  $\theta_T$  and  $\theta_S$  are found within a required accuracy. It should be pointed out that this iterative process works only for small values of  $A$ ,  $B$  and  $C$  and thus small angles  $\alpha$ ,  $\beta$ ,  $\gamma$  and  $\delta$ .

Since the tilt rotation axis is designed to lie behind the sample surface, it will move the centre of the sample surface out of the centre of the UHV chamber when the sample is tilted. Keeping the centre of the sample surface in place during tilting implies a coupling to the  $XYZ$  degrees of freedom of the manipulator. If the thickness of the sample is different from that required it must also be corrected for by  $X$ - $Y$ - $Z$  movements. The couplings of the different rotations to  $X$ - $Y$ - $Z$  are given by

$$\begin{aligned} X &= (a + d)(1 - \cos \theta_T) \cos \theta_P - d \cos \theta_P \\ &= [a - (a + d) \cos \theta_T] \cos \theta_P \end{aligned} \quad (20)$$

$$\begin{aligned} Y &= (a + d)(1 - \cos \theta_T) \sin \theta_P - d \sin \theta_P \\ &= [a - (a + d) \cos \theta_T] \sin \theta_P \end{aligned} \quad (21)$$

$$Z = (a + d) \sin \theta_T = (a + d) \sin \theta_T \quad (22)$$

with  $a$  the distance between the tilt rotation axis and the sample surface reference plane and  $d$  the distance of the sample surface from this reference plane ( $d > 0$  for a thicker sample than required).

With the mathematics described it is possible to determine the manipulator and detector positions for a given set of experimental angles  $\theta_i$ ,  $\phi_i$ ,  $\theta_f$  and  $\phi_f$ . The mathematical procedure is implemented in computer software.

## 6. Conclusions

We have given a description of a sample manipulator with three translational and three rotational degrees of freedom. Two angles describing the direction of the incident particles can be set: one with respect to the surface normal and one with respect to a reference direction on the sample surface. In combination with a detector, which can be rotated in one plane, particles leaving the surface both in and out of the

incidence plane can be detected. A mathematical procedure for these movements is derived. The accuracy of the positioning is determined by the accuracy of the calibration procedure rather than by the resolution and reproducibility of the manipulator and detector.

The mounted sample can be cooled with liquid N<sub>2</sub> and heated to temperatures of at least 1600 K by radiation and electron bombardment. At the lowest temperature the sample can still be set to another position.

### Acknowledgments

The development of the sample manipulator was carried out in the research programme of the Stichting voor Fundamenteel Onderzoek der Materie (FOM, Foundation for Fundamental Research on Matter) and was made possible by financial support from the Nederlandse Organisatie voor Wetenschappelijk Onderzoek (NWO, Dutch Organisation for Advancement of Research). The help of the late Frans Vitalis in solving the mathematical equations is acknowledged. Ron Heeren and David Butler are thanked for their critical reading of the manuscript.

### References

- [1] Raukema A, Dirksen R J and Kleyn A W 1995 Probing the (dual) repulsive wall in the interaction of O<sub>2</sub>, N<sub>2</sub> and Ar with the Ag(111) surface *J. Chem. Phys.* **103** 6217–31
- [2] Tenner M G, Kuipers E W, Langhout W Y, Kleyn A W, Nicolassen G and Stolte S 1990 Molecular beam apparatus to study interactions of oriented NO and surfaces *Surf. Sci.* **236** 151–68
- [3] Geuzebroek F H, Wiskerke A E, Tenner M G, Kleyn A W, Stolte S and Namiki A 1991 Rotational excitation of orientated molecules as a probe of molecule–surface interaction *J. Chem. Phys.* **95** 8409–21
- [4] King D A, and Wells M G 1972 Molecular beam investigation of adsorption kinetics on bulk metal targets: nitrogen on tungsten *Surf. Sci.* **29** 454–82
- [5] Raukema A, Butler D A and Klyen A W 1996 The interaction of oxygen with the Ag(110) surface *J. Phys.: Condens. Matter* **8** 2247–63
- [6] Raukema A, Butler D A and Klyen A W 1997 O<sub>2</sub> transient trapping–desorption at the Ag(111) surface *J. Chem. Phys.* accepted for publication
- [7] Raukema A, Butler D A, Box F M A and Kleyn A W 1996 Dissociative and non-dissociative sticking of O<sub>2</sub> at the Ag(111) surface *Surf. Sci.* **347** 151–68
- [8] Arfken G 1985 *Mathematical Methods for Physicists* (San Diego, CA: Academic)